

Differential study of DCE-MRI parameters in spinal metastatic tumors, brucellar spondylitis and spinal tuberculosis

Pengfei Qiao*, Pengfei Zhao*, Yang Gao, Yuzhen Bai, Guangming Niu

Department of Magnetic Resonance Imaging, the Affiliated Hospital of Inner Mongolia Medical University, Hohhot 010050, China

*These authors contributed equally to this work.

Correspondence to: Guangming Niu. Department of Magnetic Resonance Imaging, the Affiliated Hospital of Inner Mongolia Medical University, Hohhot 010050, China. Email: 24853170@qq.com.

Abstract

Objective: In the present study, spinal metastatic tumors, brucellar spondylitis and spinal tuberculosis were quantitatively analyzed using dynamic contrast-enhanced magnetic resonance imaging (DCE-MRI) to assess the value of DCE-MRI in the differential diagnosis of these diseases.

Methods: Patients with brucellar spondylitis, spinal tuberculosis or a spinal metastatic tumor (30 cases of each) received conventional MRI and DCE-MRI examination. The volume transfer constant (K^{trans}), rate constant (K_{ep}), extravascular extracellular volume fraction (V_e) and plasma volume fraction (V_p) of the diseased vertebral bodies were measured on the perfusion parameter map, and the differences in these parameters between the patients were compared.

Results: For pathological vertebrae in cases of spinal metastatic tumor, brucellar spondylitis and spinal tuberculosis, respectively, the K^{trans} values (median \pm quartile pitch) were 0.989 ± 0.014 , 0.720 ± 0.011 and $0.317 \pm 0.005 \text{ min}^{-1}$; the K_{ep} values were 2.898 ± 0.055 , 1.327 ± 0.017 and $0.748 \pm 0.006 \text{ min}^{-1}$; the V_e values were 0.339 ± 0.008 , 0.542 ± 0.013 and 0.428 ± 0.018 ; the V_p values were 0.048 ± 0.008 , 0.035 ± 0.004 and 0.028 ± 0.009 ; the corresponding H values were 50.25 (for K^{trans}), 52.47 (for K_{ep}), 48.33 (for V_e) and 46.56 (for V_p), and all differences were statistically significant (two-sided $P < 0.05$).

Conclusions: The quantitative analysis of DCE-MRI has a certain value in the differential diagnosis of spinal metastatic tumor, brucellar spondylitis and spinal tuberculosis.

Keywords: Differential diagnosis; dynamic contrast enhanced MRI; spinal tuberculosis; spinal metastatic tumor; brucellar spondylitis

Submitted Nov 15, 2017. Accepted for publication May 10, 2018.

doi: 10.21147/j.issn.1000-9604.2018.04.05

View this article at: <https://doi.org/10.21147/j.issn.1000-9604.2018.04.05>

Introduction

Spinal metastatic tumor and spinal tuberculosis are common diseases of the spine (1). The typical manifestations of spinal tuberculosis are vertebral bone destruction, intervertebral disc space reduction and paravertebral abscess; and the manifestations of spinal metastatic tumor typically include bone destruction and presence of a soft tissue mass, which rarely invades the intervertebral disc (2).

Brucellosis, a disease that typically invades the spine and often causes vertebral infection, is endemic in the pasturing areas of the Inner Mongolia Autonomous Region of China, where its incidence rate is markedly higher compared with other areas. As some patients lack the relevant epidemiological history and blood test results, it is often difficult to distinguish this disease from spinal tuberculosis and spinal metastasis by routine imaging examination.

When inflammatory diseases such as brucellar spondylitis or spinal tuberculosis are in the early stages,

diffuse inflammatory edema in the diseased vertebral bodies is often the only manifestation, and the typical abscesses may not yet be present, rendering it impossible to distinguish between these two diseases. With the progression of the disease, the vertebral body is gradually destroyed, and soft tissue is observed adjacent to the vertebral column. Furthermore, paravertebral lesions manifest as solid masses when brucellar spondylitis and spinal tuberculosis have not yet involved the intervertebral disc, and it is therefore difficult to determine whether soft tissue lesions are metastatic tumors (3-7). As these three diseases are treated differently, the correct preoperative diagnosis greatly aids in determining the appropriate treatment regimen and optimal treatment approach (8).

In the present study, the parameters of dynamic contrast-enhanced magnetic resonance imaging (DCE-MRI) of the spine in patients with spinal metastatic tumor, brucellar spondylitis or spinal tuberculosis was quantitatively analyzed in order to explore the value of DCE-MRI in the differential diagnosis of these three diseases.

Materials and methods

Patients

The present study included 30 patients with brucellar spondylitis who had complete biochemical test data or surgical information (19 males, 11 females; mean age, 50 years old); 30 patients with spinal tuberculosis (20 males, 10 females; mean age, 44 years old); and 30 patients with spinal metastatic tumor (16 males, 14 females; mean age, 60 years old). All the patients were admitted to the Department of Magnetic Resonance Imaging of the First Affiliated Hospital of Inner Mongolia Medical University between September 2015 and August 2016, with clinical manifestations of intermittent or persistent backache, and restricted movement with or without low-grade fever and night sweats. The diagnoses were confirmed by biochemical tests, surgery or pathological examinations, and patients provided written informed consent for the MRI examinations. All patients received routine MRI and DCE-MRI examination in Department of Magnetic Resonance Imaging.

Inspection equipment and scanning

All examinations were performed with a superconducting magnetic resonance scanner (Discovery MR750 3.0 T; GE Healthcare, Chicago, IL, USA) in the Department of

Magnetic Resonance Imaging. Firstly, routine MRI examination of the whole spine was performed using a phased-array surface coil, including the following: Sagittal fast-recovery fast spin-echo (FRFSE)-T2-weighted imaging (T2WI) [repetition time (TR)=3,942 ms; echo time (TE)=122 ms; echo train length (ETL)=21], fast spin-echo (FSE)-T1-weighted imaging (T1WI) (TR=608 ms; TE=8 ms; ETL=5), and FRFSE-short T1 inversion recovery (TR=3,627 ms; TE=105 ms; ETL=17), with section thickness 4.0 mm, interlayer spacing 0.5 mm, and scanning field-of-view (FOV) 320 mm × 320 mm; and axial FSE-T2WI (TR=4,830 ms; TE=129 ms; ETL=21), with section thickness 3.5 mm, interlayer spacing 0.5 mm, and scanning FOV 200 mm × 200 mm.

LAVA-XV (3-dimensional gradient echo-T1WI) sequences (GE Healthcare) were adopted for T1W-DCE-MRI; multi-flip-angle scanning was performed prior to dynamic enhancement scanning, and there were a total of four flip-angle sequences, each of which was scanned by one phase. The flip angles included 5°, 8°, 10° and 15°, and the scanning parameters were as follows: Section thickness 5.0 mm, TR=3.0 ms, TE=1.3 ms, scanning FOV 380 mm × 380 mm, and scanning matrix 256×170. Dynamically enhanced scanning was performed after multi-flip-angle scanning, using the following parameters: Section thickness 5.0 mm, TR=3.0 ms, TE=1.3 ms, flip angle 15°, scanning FOV 380 mm × 380 mm, and matrix 256×170. Omniscan (GE Healthcare) was injected through an elbow vein trocar (20 G) using magnetic resonance pressure syringe (MEDRAD Spectris Solaris EP MR Injection System, Bayer HealthCare LLC, Whippany, NJ, USA) at a dose of 0.2 mmol/kg and a flow rate of 3 mL/s, and the connection tube was immediately flushed using 20 mL of normal saline at the same flow rate. LAVA-XV dynamically enhanced scan sequences were initiated when the contrast agent injection was started, and the vertebral bodies were scanned by multi-phase (total 38 phases) dynamic continuous scanning, lasting 8 s per phase.

DCE-MRI quantitative parameter calculation

The T1W-DCE-MRI scans were processed using Omni-Kinetics software 13.0 (GE Healthcare), and the vertebral body lesion area was drawn in quasi-circular regions of interest (ROIs) with a size of 2.0–3.0 cm². The volume transfer constant (K^{trans}), extravascular extracellular volume fraction (V_e), intravascular volume fraction (V_p), and the rate constant (K_{ep}) of contrast agent returning from the

extravascular extracellular space (EES) to the plasma ($K_{ep}=K^{trans}/V_e$) in each ROI were measured, and then the mean value of each parameter was calculated.

The individual artery input function was obtained from an ROI drawn on the abdominal aorta located in close proximity to the ileocecal valve. One ROI of each chosen vertebra was drawn, with a size of 2.1–3.2 cm², and the extended Tofts linear model was selected for analyzing the values of the four DCE-MRI parameters. Each ROI was located in the vertebral body, with the adjacent vertebral artery and vertebral abscess avoided as far as possible; the ROI of each lesion was measured three times by the same researcher to calculate the mean values.

Statistical analysis

The values of perfusion parameters K^{trans} , K_{ep} , V_e and V_p were expressed as the median \pm quartile pitch, and were statistically analyzed using SPSS 17.0 software (SPSS Inc., Chicago, IL, USA). The intergroup differences in the parameters were calculated by the Kruskal Wallis H test, and statistical significance was set at two-sided $P < 0.05$.

Results

Number of lesions, disease location and conventional MRI performance

In total, 90 patients were enrolled in the present study. Among the 30 patients with brucellar spondylitis, there were 25 cases of lumbosacral vertebral lesion (83%), 4 cases of thoracic vertebral lesion (13%) and 1 case of cervical vertebral lesion (3%); in the lumbosacral vertebral lesions, the L5 and S1 vertebrae were most commonly involved (55%). Among the 30 patients with spinal tuberculosis, there were 17 cases of lumbosacral vertebral lesion (57%) and 13 cases of thoracic vertebral lesion (43%); in the lumbosacral vertebrae lesions, L2 and L3 were usually involved (53%). Among the 30 patients with spinal metastatic tumors, lesions frequently involved multiple vertebral bodies, and magnetic resonance signal performance varied.

The conventional MRI findings of spinal metastatic tumors showed that the lesions involved the vertebral bodies, or vertebral bodies and appendices, whereas the intervertebral disc was not involved, and the lesion signals were diverse; and on enhanced scanning, marginal or obvious enhancement was present (Figure 1A, B). The conventional MRI findings of brucellar spondylitis were as

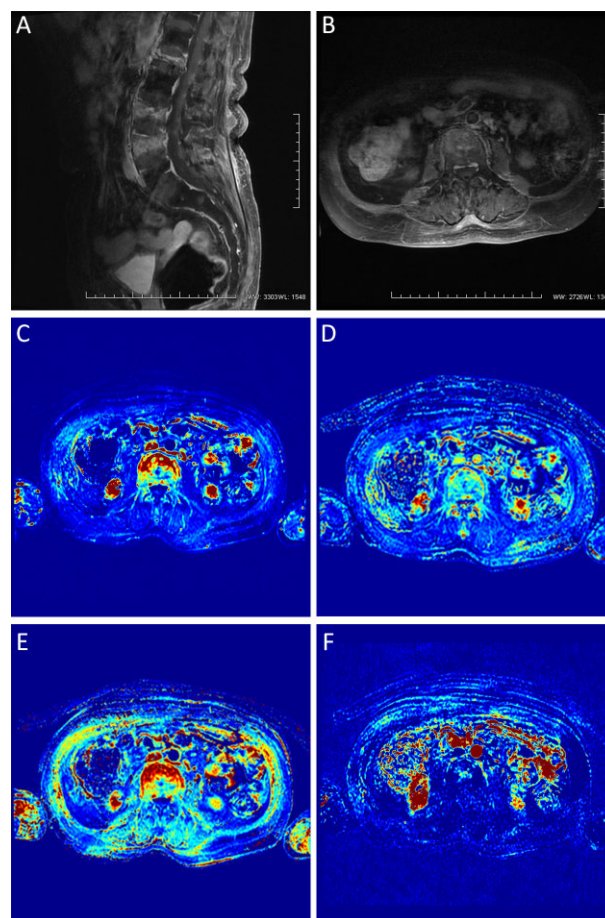


Figure 1 T1-weighted, dynamic contrast-enhanced magnetic resonance imaging (DCE-MRI) findings of a metastatic tumor in lumbar 1, 3 and 4. (A, B) Enhanced images; (C) Volume transfer constant (K^{trans}), 0.9493 min⁻¹; (D) Rate constant (K^{trans}/V_e) (K_{ep}), 2.9124 min⁻¹; (E) Extravascular extracellular volume (V_e), 0.3412; (F) Intravascular volume (V_p), 0.0476.

follows: absent or mild alterations in the morphology of the diseased vertebral bodies, manifesting as bone destruction and bone hyperplasia; in the involved area, T1WI showed low signal intensity, T2WI showed mixed signal intensity, and STIR showed homogeneous or heterogeneous high signal intensity; and on enhanced scanning, the lesions were markedly enhanced and the vertebral peripheral abscesses were localized (Figure 2A, B). The conventional MRI findings of spinal tuberculosis were as follows: the morphologies of the affected vertebral bodies were usually altered, the bones exhibited serious damage, and the intervertebral spaces were markedly narrowed or had disappeared; and on enhanced scanning, the lesions were typically circularly enhanced, and the vertebral peripheral

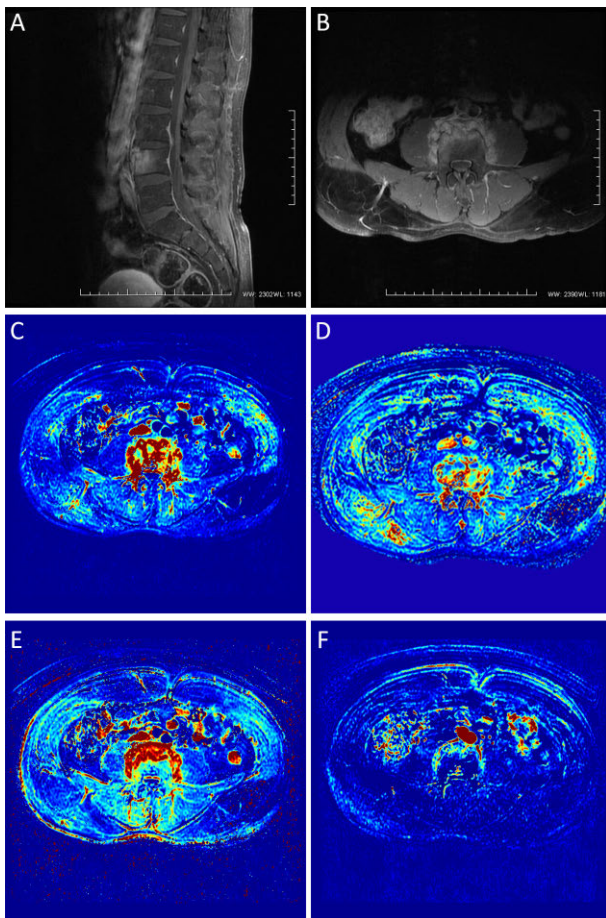


Figure 2 T1-weighted, dynamic contrast-enhanced magnetic resonance imaging (DCE-MRI) findings of brucellar spondylitis in lumbar 4 and 5. (A, B) Enhanced images; (C) Volume transfer constant (K^{trans}), 0.7080 min^{-1} ; (D) Rate constant (K^{trans}/V_e) (K_{ep}), 1.2765 min^{-1} ; (E) Extravascular extracellular volume (V_e), 0.5546 ; (F) Intravascular volume (V_p), 0.0311 .

abscesses were obvious and extensive (*Figure 3A, B*).

There were significant differences in K^{trans} , K_{ep} , V_e and V_p between different types of spondylitis, with significant differences in any pairwise comparison. K^{trans} , K_{ep} and V_p values of spinal metastases were the highest, followed by brucellosis spondylitis and spinal tuberculosis; V_e value of spinal metastases was the lowest (*Figure 1C–F*), and then spinal tuberculosis (*Figure 3C–F*) and brucellosis sequentially (*Figure 2C–F, Table 1*).

Discussion

Using plain imaging and conventional enhancement, it is challenging to distinguish inflammatory granuloma from metastatic soft tissue masses, and to distinguish benign

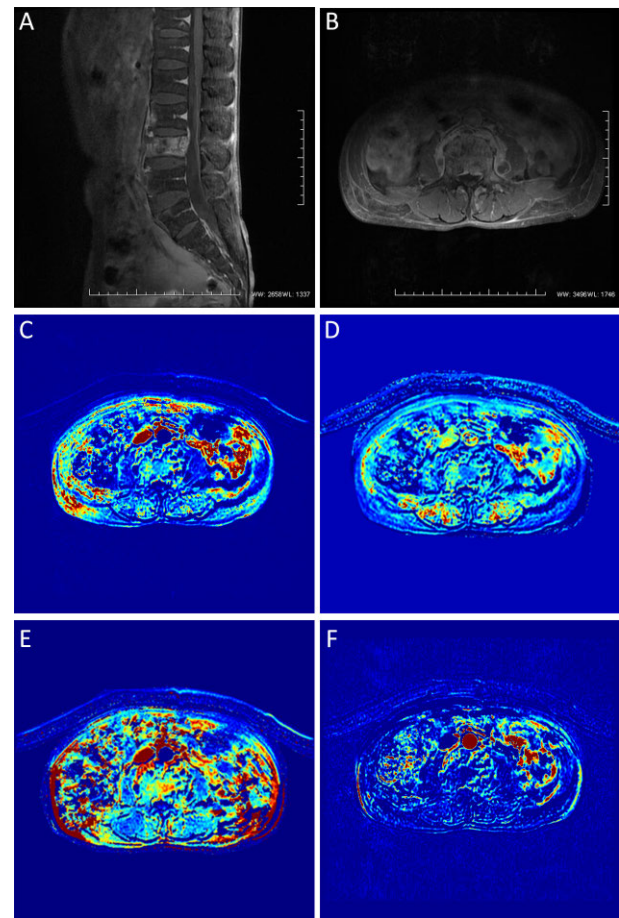


Figure 3 T1-weighted, dynamic contrast-enhanced magnetic resonance imaging (DCE-MRI) findings of spinal tuberculosis in lumbar 3 and 4. (A, B) Enhanced images; (C) Volume transfer constant (K^{trans}), 0.3181 min^{-1} ; (D) Rate constant (K^{trans}/V_e) (K_{ep}), 0.7589 min^{-1} ; (E) Extravascular extracellular volume (V_e), 0.4192 ; (F) Intravascular volume (V_p), 0.0287 .

spinal lesions from malignant ones if the lesions involve vertebral bone destruction, a localized mass, no disc involvement or no paravertebral abscess (3–5). Furthermore, it is often challenging to identify the causes of bone marrow edema, or to distinguish between different types of inflammatory lesions when the lesions manifest as vertebral bone marrow edema with no vertebral destruction, no disc involvement or no paravertebral abscess (9,10).

Malignant tumors require angiogenesis to maintain their growth and invasion, and these new vessels are distributed abnormally, with uneven diameters and loose junctions between the endothelial cells. By contrast, in inflammatory lesions, the vascular structures are mature, and the main

Table 1 Perfusion parameters for different types of spinal lesions

| Index | No. of cases | K^{trans} (min^{-1}) | K_{ep} (min^{-1}) | V_e | V_p |
|-------------------------|--------------|--|---------------------------------------|-------------|-------------|
| Spinal metastatic tumor | 30 | 0.989±0.014 | 2.898±0.055 | 0.339±0.008 | 0.048±0.008 |
| Brucellar spondylitis | 30 | 0.720±0.011 | 1.327±0.017 | 0.542±0.013 | 0.035±0.004 |
| Spinal tuberculosis | 30 | 0.317±0.005 | 0.748±0.006 | 0.428±0.018 | 0.028±0.009 |
| H | | 50.25 | 52.47 | 48.33 | 46.56 |
| P | | <0.05 | <0.05 | <0.05 | <0.05 |

K^{trans} , volume transfer constant; K_{ep} , rate constant (K^{trans}/V_e); V_e , extravascular extracellular volume; V_p , intravascular volume. The parameter values are expressed as median ± quartile pitch, and the intergroup differences were calculated by Kruskal Wallis H test.

manifestation is vascular dilatation rather than angiogenesis. Therefore, different types of lesions may exhibit different DCE-MRI dynamic features. Overall, the DCE features in cases of metastatic tumors, as compared with inflammatory diseases, reflect the higher contrast agent activity in the internal and external invading vessels (11-13). To the best of our knowledge, although DCE-MRI has been widely used in the evaluation of many types of tumors, there have been no reports of the use of DCE-MRI to identify patients with brucellar spondylitis, spinal tuberculosis and spinal metastatic tumors. In the present study, the three diseases had significantly distinctive DCE-MRI dynamics, indicating that they differ with regard to vascular permeability and spatial distribution.

Spinal metastatic tumors, brucellar spondylitis and spinal tuberculosis differ, and thus the correct imaging diagnosis is extremely helpful in selecting the most appropriate treatment protocol. Brucellar spondylitis is predominantly treated conservatively with medication; spinal tuberculosis is primarily treated by anti-tuberculosis therapy or surgery; and metastatic tumor patients may receive additional examinations to determine the primary cancer and to select the best treatment strategy for the metastases (which may include surgery, radiotherapy or chemotherapy) (14-16).

The pathological manifestations of tuberculosis include exudation, proliferation and caseous necrosis, while brucellar spondylitis manifests as exudation, proliferation and granuloma, suggesting that spinal tuberculosis and brucellosis spondylitis have more tissue space for the retention of MRI contrast agent (17-19). However, spinal metastatic tumors may have higher cell density and less tissue space, manifesting distinctive pathological features, such as abnormal blood vessels and cells; therefore, the DCE dynamic performance may be more active. As mentioned, the common pathological features of brucellar spondylitis and spinal tuberculosis include exudation and proliferation, and the difference between them is that the

former shows granuloma and the latter shows caseous necrosis. This may explain why the former shows more aggressive DCE dynamics.

The DCE-MRI quantitative parameters applied in this study included K^{trans} , K_{ep} , V_e , and V_p . Greater values of K^{trans} (the transfer rate of contrast agent from blood to tissue space) indicate higher vascular permeability and more serious injury of endothelial cells. The transfer rate of the contrast agent from the tissue space to the blood is expressed by K_{ep} . The contrast agent volume per unit volume of tissue extracellular space is represented by V_e ; the greater the value of V_e , the larger the tissue extracellular space, indicating a higher degree of necrosis or lower cell density. V_p represents the volume of plasma per unit volume of tissue, and the relationship between V_p and V_e is such that $V_p+V_e \leq 1$ (20,21).

In the present study, the K^{trans} , K_{ep} and V_p values were highest in spinal metastatic tumors, followed by brucellar spondylitis and spinal tuberculosis, while the V_e value was lowest in spinal metastatic tumors, followed by spinal tuberculosis and brucellar spondylitis. This suggested that increased angiogenesis, vascular endothelial cell damage or immaturity, as well as cell genesis, were most significant in spinal metastatic tumor lesions, whereas such manifestations were the least significant in tuberculosis. Thus, the results were consistent with the pathological basis of the three diseases. The disease course and conditions of brucellar spondylitis are complex, resulting in the discrete distribution of DCE-MRI parameters at different stages of the disease due to different pathological changes and degrees of vascular permeability. The differences in the quantitative parameters among the three diseases have been identified in typical cases in the present study. However, in atypical cases, the values of quantitative parameters in brucellar spondylitis can be similar to those in spinal tuberculosis and spinal metastatic tumors; thus, further research with a larger number of cases is required

to fully clarify the differences and determine the role of DCE-MRI quantitative analysis in the diagnosis of spinal lesions, and thereby to provide more reliable and accurate diagnostic evidence of atypical spinal lesions.

Conclusions

The current study shows imaging findings from cases of spinal metastatic tumors, brucellar spondylitis and spinal tuberculosis. These three cases did not exhibit the typical features of the three diseases on routine plain scans and conventional enhanced scans; however, the quantitative analysis of DCE-MRI parameters provided new information to describe the changes in vertebral body microstructure and bone marrow perfusion, thus providing a reliable basis for the diagnosis of these three diseases when routine plain scans and conventional enhanced scans fail to give the correct diagnosis.

Acknowledgements

This study was funded by the National Natural Science Foundation of China (No. 81460259).

Footnote

Conflicts of Interest: The authors have no conflicts of interest to declare.

References

1. Go SW, Lee HY, Lim CH, et al. Atypical disseminated skeletal tuberculosis mimicking metastasis on PET-CT and MRI. *Intern Med* 2012; 51:2961-5.
2. Yu Y, Wang X, Du B, et al. Isolated atypical spinal tuberculosis mistaken for neoplasia: case report and literature review. *Eur Spine J* 2013;22:S302-5.
3. Zheng CY, Liu DX, Luo SW, et al. Imaging presentation highly manifested as tuberculosis in a case of spinal metastatic carcinoma. *Orthopedics* 2011;34:e436-8.
4. Cui EB, Bao CM, Guo TS, et al. Epidemic trend and diagnosis of brucellosis. *Chuan Ran Bing Xin Xi* (in Chinese) 2010;23:20-22.
5. Tali ET, Koc AM, Oner AY. Spinal brucellosis. *Neuroimaging Clin N Am* 2015;25:233-45.
6. Lang N, Su MY, Yu HJ, et al. Differentiation of tuberculosis and metastatic cancer in the spine using dynamic contrast-enhanced MRI. *Eur Spine J* 2015;24:1729-37.
7. Saltoglu N, Tasova Y, Inal AS, et al. Efficacy of rifampicin plus doxycycline versus rifampicin plus quinolone in the treatment of brucellosis. *Saudi Med J* 2002;23:921-4.
8. Andriopoulos P, Tsironi M, Deftereos S, et al. Acute brucellosis: presentation, diagnosis, and treatment of 144 cases. *Int J Infect Dis* 2007;11:52-7.
9. Ge Z, Wang Z, Wei M. Measurement of the concentration of three antituberculosis drugs in the focus of spinal tuberculosis. *Eur Spine J* 2008; 17:1482-7.
10. Jin D, Qu D, Chen J, et al. One-stage anterior interbody autografting and instrumentation in primary surgical management of thoracolumbar spinal tuberculosis. *Eur Spine J* 2004;13:114-21.
11. Lebre A, Velez J, Seixas D, et al. Brucellar spondylodiscitis: case series of the last 25 years. *Acta Med Port* 2014;27:204-10.
12. Rock JP, Ryu S, Yin FF, et al. The evolving role of stereotactic radiosurgery and stereotactic radiation therapy for patients with spine tumors. *J Neurooncol* 2004;69:319-34.
13. Parker GJ, Roberts C, Macdonald A, et al. Experimentally-derived functional form for a population-averaged high-temporal-resolution arterial input function for dynamic contrast-enhanced MRI. *Magn Reson Med* 2006;56:993-1000.
14. Tokuda O, Hayashi N, Taguchi K, et al. Dynamic contrast-enhanced perfusion MR imaging of diseased vertebrae: analysis of three parameters and the distribution of the time-intensity curve patterns. *Skeletal Radiol* 2005;34:632-8.
15. Qiao P, Niu H, Bai Y, et al. The differential diagnosis value of DCE-MRI in brucellosis spondylitis. *He Ci Gong Zhen Cheng Xiang* (in Chinese) 2015;6:581-4.
16. Pourbagher A, Pourbagher MA, Savas L, et al. Epidemiologic, clinical, and imaging findings in brucellosis patients with osteoarticular involvement. *AJR Am J Roentgenol* 2006;187:873-80.
17. Jin D, Qu D, Chen J, et al. One-stage anterior interbody autografting and instrumentation in primary surgical management of thoracolumbar spinal tuberculosis. *Eur Spine J* 2004;13:114-21.

18. Wu X, Niu G, Gao Y. Research progress of magnetic resonance imaging in brucellosis spondylitis. *He Ci Gong Zhen Cheng Xiang* (in Chinese) 2017;8:317-20.
19. Nazarpour M, Poureisa M, Daghighi MH. Comparison of maximum signal intensity of contrast agent on t1-weighted images using spin echo, fast spin echo and inversion recovery sequences. *Iran J Radiol* 2012;10:27-32.
20. Wang XY, Yan F, Hao H, et al. Improved performance in differentiating benign from malignant sinonasal tumors using diffusion-weighted combined with dynamic contrast-enhanced magnetic resonance imaging. *Chin Med J (Engl)* 2015;128:586-92.
21. Niu H, Gao Y, Qiao P, et al. Dynamic contrast-enhanced MRI in the early diagnosis of brucella spondylitis. *Zhonghua Fang She Xue Za Zhi* (in Chinese) 2017;51:437-40.

Cite this article as: Qiao P, Zhao P, Gao Y, Bai Y, Niu G. Differential study of DCE-MRI parameters in spinal metastatic tumors, brucellar spondylitis and spinal tuberculosis. *Chin J Cancer Res* 2018;30(4):425-431. doi: 10.21147/j.issn.1000-9604.2018.04.05